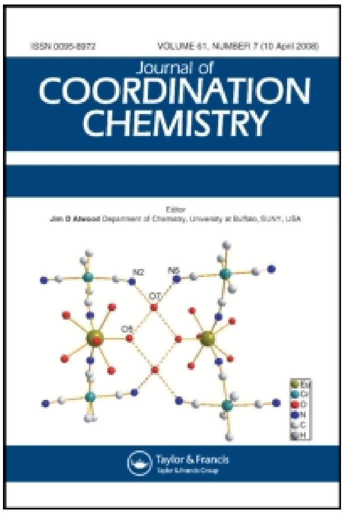

Journal of Coordination Chemistry
Publication details, including instructions for authors and subscription information:
http://www.informaworld.com/smpp/title~content=t713455674

Synthesis, characterization, and antimicrobial studies of some Schiff-base metal(II) complexes

Chellaian Justin Dhanaraj[a]; Madhavan Sivasankaran Nair[a]
[a] Department of Chemistry, Manonmaniam Sundaranar University, Tirunelveli 627 012, Tamil Nadu, India

To cite this Article Dhanaraj, Chellaian Justin and Nair, Madhavan Sivasankaran(2009) 'Synthesis, characterization, and antimicrobial studies of some Schiff-base metal(II) complexes', Journal of Coordination Chemistry, 62: 24, 4018 — 4028, First published on: 22 September 2010 (iFirst)

To link to this Article: DOI: 10.1080/00958970903191142

URL: http://dx.doi.org/10.1080/00958970903191142

Journal of Coordination Chemistry
Vol. 62, No. 24, 20 December 2009, 4018–4028

Taylor & Francis
Taylor & Francis Group

Synthesis, characterization, and antimicrobial studies of some Schiff-base metal(II) complexes

CHELLAIAN JUSTIN DHANARAJ and
MADHAVAN SIVASANKARAN NAIR*

Department of Chemistry, Manonmaniam Sundaranar University,
Tirunelveli 627 012, Tamil Nadu, India

(*Received 25 October 2008; in final form 8 June 2009*)

Neutral complexes of Co(II), Ni(II), Cu(II), and Zn(II) have been synthesized from the Schiff bases derived from 3-nitrobenzylidene-4-aminoantipyrine and aniline (L^1)/*p*-nitro aniline (L^2)/*p*-methoxy aniline (L^3) in the molar ratio 1 : 1. The structural features have been determined from microanalytical, IR, UV-Vis, ^{1}H-NMR, mass, and ESR spectral data. The Cu(II) complexes are square planar, while Co(II), Ni(II), and Zn(II) complexes are tetrahedral. Magnetic susceptibility measurements and molar conductance data provide evidence for the monomeric and neutral nature of the complexes. The X-band ESR spectrum of Cu(II) complexes at 300 and 77 K were recorded. The electrochemical behavior of the complexes in MeCN at 298 K was studied. The *in vitro* biological screening effects of the investigated compounds were tested against the bacterial species *Staphylococcus aureus*, *Escherichia coli*, *Klebsiella pneumoniae*, *Proteus vulgaris*, and *Pseudomonas aeruginosa* and fungal species *Aspergillus niger*, *Rhizopus stolonifer*, *Aspergillus flavus*, *Rhizoctonia bataicola*, and *Candida albicans* by the well-diffusion method. Comparison of the inhibition values of the Schiff bases and their complexes indicate that the complexes exhibit higher antimicrobial activity.

Keywords: Schiff base; IR; UV-Vis; Mass; ESR; Biological screening

1. Introduction

The Schiff bases are widely studied because of the increasing recognition of their role in biological systems [1]. Mononuclear complexes of acyclic Schiff-base ligands have been reported [2]. Schiff-base complexes are used as catalysts in some chemical processes, as biological models for understanding the structures of biomolecules and to emulate the activity of proteins [3].

In azomethine derivatives, the C=N linkage is essential for biological activity; several azomethines were reported to possess remarkable antibacterial [4–6], antifungal [7, 8], anticancer [9, 10], and diuretic activities [11]. With the increasing incidence of deep mycosis, there has been increasing emphasis on the screening of new and more effective antimicrobial drugs with low toxicity. Schiff bases and their complexes were recently found to have significant antitumor and biological activity [12, 13].

---

*Corresponding author. Email: msnairchem@rediffmail.com

Journal of Coordination Chemistry
ISSN 0095-8972 print/ISSN 1029-0389 online © 2009 Taylor & Francis
DOI: 10.1080/00958970903191142

Antipyrine derivatives are reported to exhibit analgesic and anti-inflammatory effects [14, 15], antiviral [16], antibacterial [17], and herbicidal [18] activities, and have also been used as hair color additives and to potentiate the local anesthetic effect of Lidocaine [19]. Transition metal complexes with ligands derived from 4-aminoantipyrine have significant biological activity [20]. This prompted us to synthesize a new series of heterocyclic Schiff bases containing the antipyrinyl moiety. The present article reports the results on Co(II), Ni(II), Cu(II), and Zn(II) complexes of Schiff bases derived from 3-nitrobenzylidene-4-aminoantipyrine and aniline (L^1)/*p*-nitro aniline (L^2)/*p*-methoxy aniline (L^3) in molar ratio 1 : 1.

2. Experimental

2.1. *Materials*

The chemicals used were of AnalaR grade. 4-Aminoantipyrine and metal(II) acetates were obtained from Sigma and Merck. Acetonitrile was dried over phosphorous pentoxide and distilled repeatedly to obtain a highly pure product.

2.2. *Synthesis of Schiff bases*

3-Nitrobenzylidene-4-aminoantipyrine was prepared by the condensation of 3-nitrobenzaldehyde and 4-aminoantipyrine. An ethanolic solution of 3-nitrobenzylidene-4-aminoantipyrine and aniline (L^1)/*p*-nitro aniline (L^2)/*p*-methoxy aniline (L^3) (0.01 mol) was refluxed for *ca* 6 h. The solvent was then reduced to one-third of its volume and the resulting solution was cooled to 0°C. The solid product formed (scheme 1) was removed by filtration and recrystalized from ethanol.

2.3. *Synthesis of metal(II) complexes*

In order to avoid the hydrolysis of Schiff bases, they were kept below pH 4 [21] by adding hydrochloric acid. A solution of metal(II) acetates and the Schiff bases (0.01 mol) in ethanol (50 mL) was stirred for *ca* 3 h using a magnetic stirrer. The precipitated complex was filtered, washed with hot distilled water, followed by ethanol and dried in vacuum. The Schiff bases and their metal complexes were characterized by microanalytical and spectroscopic methods.

2.4. *Physical measurements*

Elemental analyses of the ligands and their metal complexes were carried out using a Perkin-Elmer elemental analyzer. The amount of metal present in the metal complexes was estimated using the ammonium oxalate method [22]. Molar conductances of the metal complexes were measured in a DMSO solution using a Coronation digital conductivity meter. Magnetic susceptibility values were calculated using the relation $\mu_{\text{eff}} = 2.83\ (\chi_{\text{m}} \cdot T)$. IR spectra were recorded in KBr discs on a JASCO FT/IR-410 spectrometer from 4000 to 400 cm^{-1}. Electronic spectra were recorded with a

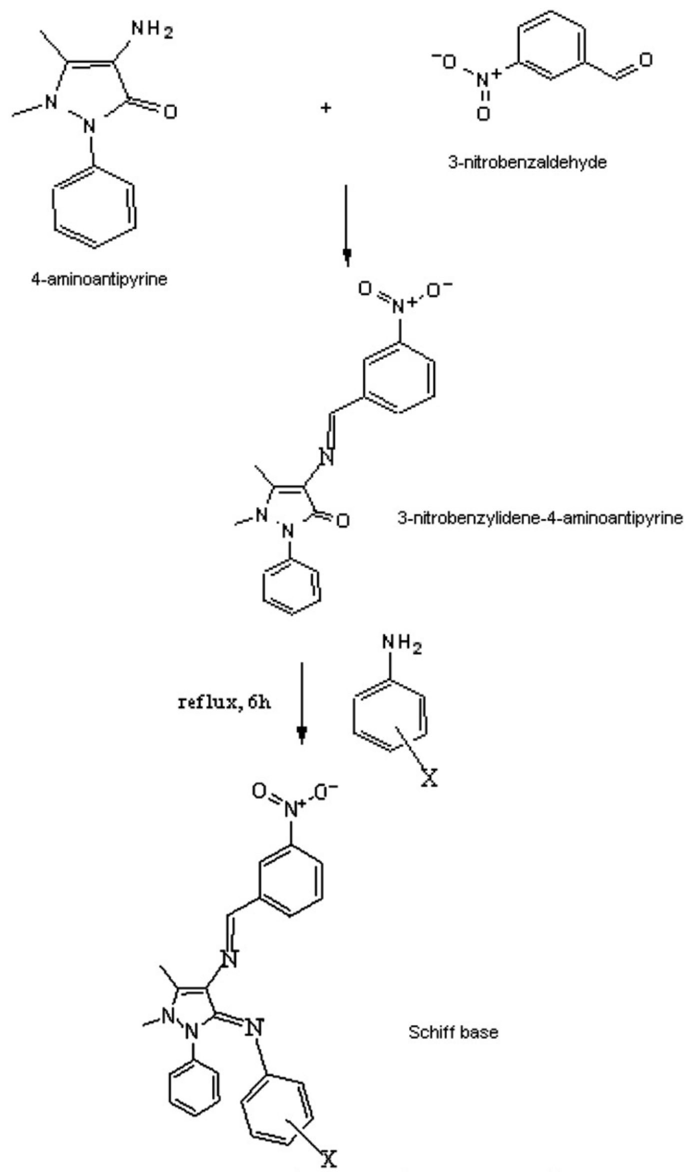

where X = H (L^1), p-NO_2 (L^2) and p-OCH_3 (L^3)

Scheme 1. Synthesis of Schiff base ligands.

Perkin-Elmer Lambda-25 UV-Vis spectrometer from 200 to 1100 nm. ^1H-NMR spectra were recorded with a Brucker 300 MHz NMR spectrometer using $CDCl_3$ for ligands and DMSO-d_6 for Zn(II) complexes with TMS as internal standard. FAB mass spectra were recorded on a JEOL SX 102/DA-6000 mass spectrometer/data system using argon/xenon (6 kV, 10 mA) as the FAB gas. The accelerating voltage was 10 kV and the spectra were recorded at room temperature using *m*-nitrobenzyl alcohol (NBA) as the matrix. ESR spectra of the Cu(II) complexes were recorded at 300 and 77 K in a DMSO solution using a Varian E112 X-band spectrometer. Cyclic voltammetric measurements were performed using a glassy carbon working electrode, Pt wire auxiliary electrode and an Ag/AgCl reference electrode. $\mathrm{LiClO_4}$ was used as the supporting electrolyte.

2.5. *Antimicrobial activity*

The *in vitro* biological screening effects of the compounds were tested against the bacterial species *Staphylococcus aureus*, *Escherichia coli*, *Klebsiella pneumoniae*, *Proteus vulgaris*, and *Pseudomonas aeruginosa* and fungal species *Aspergillus niger*, *Rhizopus stolonifer*, *Aspergillus flavus*, *Rhizoctonia bataicola*, and *Candida albicans* by the well-diffusion method [23]. Stock solution (0.001 mol) was prepared by dissolving the compounds in DMSO and the solutions were serially diluted to find the MIC values ($\mu\mathrm{g\,mL^{-1}}$). Antimicrobial activities were performed in triplicate and the average was taken as the final reading. Error limits are also indicated in the respective tables.

3. Results and discussion

All the complexes are stable at room temperature, insoluble in water, but soluble in DMSO and MeCN. Analytical data and molar conductance values for the complexes are given in table S1 (Supplementary material). The complexes showed low molar conductances (09–24 $\mathrm{mho\,cm^2\,mol^{-1}}$) indicating non-electrolytes [24].

3.1. *IR spectra*

The important IR spectral data of the free ligands and their complexes are summarized in table 1. The IR spectra of the ligands show two different characteristic >C=N bands

Table 1. IR spectral data of ligands and complexes.

Compound	$\nu_{(\mathrm{C=N})}$[a] (cm^{-1})	$\nu_{(\mathrm{C=N})}$[b] (cm^{-1})	$\nu_{\mathrm{asym(COO^-)}}$ (cm^{-1})	$\nu_{\mathrm{sym(COO^-)}}$ (cm^{-1})	$\nu_{(\mathrm{M–O})}$ (cm^{-1})	$\nu_{(\mathrm{M–N})}$ (cm^{-1})
L^1	1655	1650	–	–	–	–
$[\mathrm{CoL}^1(\mathrm{OAc})_2]$	1631	1628	1622	1329	480	435
$[\mathrm{NiL}^1(\mathrm{OAc})_2]$	1629	1627	1620	1325	485	428
$[\mathrm{CuL}^1(\mathrm{OAc})_2]$	1632	1630	1619	1323	472	440
$[\mathrm{ZnL}^1(\mathrm{OAc})_2]$	1635	1632	1618	1324	463	428
L^2	1638	1648	–	–	–	–
$[\mathrm{CoL}^2(\mathrm{OAc})_2]$	1625	1626	1616	1321	475	431
$[\mathrm{NiL}^2(\mathrm{OAc})_2]$	1626	1625	1617	1322	460	422
$[\mathrm{CuL}^2(\mathrm{OAc})_2]$	1628	1629	1619	1325	465	418
$[\mathrm{ZnL}^2(\mathrm{OAc})_2]$	1627	1628	1618	1323	450	410
L^3	1660	1652	–	–	–	–
$[\mathrm{CoL}^3(\mathrm{OAc})_2]$	1640	1632	1622	1328	490	440
$[\mathrm{NiL}^3(\mathrm{OAc})_2]$	1638	1629	1621	1326	485	437
$[\mathrm{CuL}^3(\mathrm{OAc})_2]$	1639	1631	1620	1325	488	438
$[\mathrm{ZnL}^3(\mathrm{OAc})_2]$	1637	1634	1621	1325	483	432

[a] >C=N – derived from 3-nitrobenzaldehyde.

[b] >C=N – derived from aniline/substituted anilines.

in the 1660–1638 cm^{-1} region which are shifted to lower frequencies in the spectra of the metal complexes (1640–1625 cm^{-1}). The complexes also display bands at 1622–1616 and 1328–1321 cm^{-1}, respectively, due to the asymmetric and symmetric stretching vibration of the acetate group with $\Delta\nu = 295\,cm^{-1}$, indicating the monodentate binding [25, 26]. The spectra of the metal complexes also show some new bands in the 490–450 and 440–400 cm^{-1} regions, which reflect the formation of M–O and M–N bonds [27, 28], respectively.

3.2. *Electronic spectra*

The electronic spectra of the Schiff-base ligands and their metal complexes were recorded at 300 K in MeCN. The absorption regions, assignments, and the proposed geometry of the complexes are given in table 2. These values are comparable with those of similar complexes [29]. The spectra of Co(II) complexes show bands in the 640–666 nm region, which can be attributed to $^4A_2(F) \rightarrow {}^4T_1(P)$ transition for the tetrahedral geometry [30]. The electronic spectra of Ni(II) complexes show d–d transition in the 630–655 nm region, due to $^3T_1(F) \rightarrow {}^3T_1(P)$ transition for tetrahedral

Table 2. Electronic spectral data of the complexes.

Compound	Solvent	Absorption (nm)	Band assignment	Geometry
L^1	$CHCl_3$	330	INCT	–
$[CoL^1(OAc)_2]$	CH_3CN	328	INCT	
		339	INCT	
		640	$^4A_2(F) \rightarrow {}^4T_1(P)$	Tetrahedral
$[NiL^1(OAc)_2]$	CH_3CN	315	INCT	
		340	INCT	
		630	$^3T_1(F) \rightarrow {}^3T_1(P)$	Tetrahedral
$[CuL^1(OAc)_2]$	CH_3CN	329	INCT	
		332	INCT	
		536	$^2B_{1g} \rightarrow {}^2A_{1g}$	Square-planar
L^2	$CHCl_3$	329	INCT	–
$[CoL^2(OAc)_2]$	CH_3CN	291	INCT	
		345	INCT	
		648	$^4A_2(F) \rightarrow {}^4T_1(P)$	Tetrahedral
$[NiL^2(OAc)_2]$	CH_3CN	310	INCT	
		324	INCT	
		642	$^3T_1(F) \rightarrow {}^3T_1(P)$	Tetrahedral
$[CuL^2(OAc)_2]$	CH_3CN	293	INCT	
		319	INCT	
		540	$^2B_{1g} \rightarrow {}^2A_{1g}$	Square-planar
L^3	$CHCl_3$	327	INCT	–
$[CoL^3(OAc)_2]$	CH_3CN	302	INCT	
		320	INCT	
		666	$^4A_2(F) \rightarrow {}^4T_1(P)$	Tetrahedral
$[NiL^3(OAc)_2]$	CH_3CN	301	INCT	
		328	INCT	
		655	$^3T_1(F) \rightarrow {}^3T_1(P)$	Tetrahedral
$[CuL^3(OAc)_2]$	CH_3CN	302	INCT	
		311	INCT	
		548	$^2B_{1g} \rightarrow {}^2A_{1g}$	Square-planar

Ni(II) complexes [31]. The Cu(II) complexes (536–548 nm) can be assigned to the $^2B_{1g} \rightarrow {}^2A_{1g}$ transition of square planar geometry [29]. The typical electronic spectra of Schiff base (L^1) and its copper complex are shown in figures S1 and S2 (Supplementary material).

3.3. *Magnetic measurements*

The magnetic moment values of the complexes are given in table S1. The observed magnetic moment values of Co(II) complexes lie from 4.63 to 4.86 B.M, a range found for tetrahedral Co(II) complexes [32–34]. For tetrahedral Ni(II) complexes, μ_{expected} is in the range 2.9–3.9 B.M. The observed magnetic moments of 2.96–3.10 B.M. for our Ni(II) complexes are in accord with tetrahedral, but also in the range expected for octahedral geometry.

The Cu(II) square planar complexes exhibit magnetic moments from 1.8 to 2.1 B.M. [35]. The magnetic moments obtained for the Cu(II) complexes in the present study fall in this range; however, five- and six-coordinate copper(II) species also give values in this range. The magnetic data are in accord with the proposed geometries. Zn(II) complex with d^{10} electronic configuration is diamagnetic and would have tetrahedral geometry.

3.4. *^{1}H-NMR spectra*

^{1}H-NMR spectral data of the ligands and their Zn(II) complexes are summarized in table S2 (Supplementary material). The ^{1}H-NMR spectra of L^1, L^2, and L^3 show the following signals: C_6H_5 as a multiplet at 6.9–7.5 ppm, $=C–CH_3$ at 2.0–2.6 ppm, $–N–CH_3$ at 2.9–3.5 ppm, and azomethine proton $–CH=N–$ at 9.1–9.6 ppm. The ^{1}H-NMR spectrum of Zn(II) complexes with L^1, L^2, and L^3 have the azomethine proton signal shifted downfield compared to the free ligand, suggesting the deshielding of the azomethine group due to the coordination with Zn(II). There is no appreciable change in other signals in the spectra of Zn(II) complexes. The ^{1}H-NMR spectrum of L^1 recorded in $CDCl_3$ is shown in figure S3 (Supplementary material).

3.5. *FAB mass spectra*

The spectrum of Co(II), Ni(II), Cu(II), and Zn(II) complexes of L^1, L^2, and L^3 were recorded and the spectra of L^1 ligand and its Cu(II) complex are given in figures S4 and S5 (Supplementary material). The molecular ion peak for L^1 was observed at 412 m/z, whereas molecular ion peaks of Co(II), Ni(II), Cu(II), and Zn(II)–L^1 complexes were observed, respectively, at 589, 589, 594, and 595 m/z, which confirm the stoichiometry of the metal complexes to be $[ML^1(OAc)_2]$. Moreover, all the synthesized complexes containing metal ion were confirmed by good agreement between the observed and calculated isotopic distributions [36]. Elemental analysis values are in close agreement with the values calculated from molecular formulas assigned to these complexes, which is further supported by the FAB-mass studies. Similar mass spectral behavior was observed for the Co(II), Ni(II), Cu(II), and Zn(II) complexes of L^2 and L^3.

3.6. *ESR spectra*

The ESR spectral data of Cu(II) complexes of L^1, L^2, and L^3 recorded in DMSO at 300 and 77 K are summarized in table S3 (Supplementary material). The spectrum at 300 K shows one intense absorption band at high field, which is isotropic due to the tumbling of the molecules. However, the complex in the frozen state (77 K) shows four well-resolved peaks with low intensities in the low-field region and one intense peak in the high-field region. The absence of a half-field signal in the spectrum at 1600 G due to the $m_s = \pm 2$ transitions rules out any Cu–Cu interaction. The g-tensor value of the copper complex can be used to derive the ground state. In Cu(II)L^1, the observed g-tensor values are $g_{\parallel}$ (2.256) > $g_{\perp}$ (2.052) > g_e (2.0036), suggesting the complex to have square-planar geometry. In the axial spectra, the g-values are related to the exchange interaction coupling constant, $G = [(g_{\parallel} - 2)/(g_{\perp} - 2)]$.

If the G value is larger than 4, the exchange interaction is negligible because the local tetragonal axes are aligned parallel or slightly misaligned. If the value is less than 4, the exchange interaction is considerable and the local tetragonal axes are misaligned [37]. For Cu(II)L^1 $G = 4.9$, suggesting that the local tetragonal axes are aligned parallel or slightly misaligned and consistent with a $d_{x^2-y^2}$ ground state. The observed value of 0.7571 for the in-plane σ-bonding covalency parameter, α^2 (0.7571), in Cu(II)L^1 indicates that the complex has some covalent character. The in-plane π-bonding parameter, β^2 (0. 9386), and out-of plane π-bonding parameter, γ^2 (0.719), demonstrate that there is an interaction in the out-of-plane π-bonding, whereas the in-plane π-bonding is completely ionic. Again, the observed order of orbital reduction factors: $K_{\perp}$ (0.5443) < $K_{\parallel}$ (0.7106) implies a greater contribution from out-of-plane π-bonding than in-plane π-bonding in metal–ligand bonding. The ESR spectra of Cu(II) complexes with L^2 and L^3 also show similar features.

3.7. *Cyclic voltammetry*

The cyclic voltammetric data of the Co(II), Ni(II), Cu(II), and Zn(II) complexes with L^1, L^2, and L^3 are summarized in table 3. The cyclic voltammogram of [CoL^1(OAc)$_2$] in acetonitrile at 300 K in the potential range from +0.6 to −1.2 V at a scan rate of 0.1 Vs^{-1} shows a well-defined redox process corresponding to the formation of the

Table 3. Cyclic voltammetric data of the complexes.

Complex	Couple/peak	Cathodic, E_{pc} (V)	Anodic, E_{pa} (V)	ΔE_p (V)
[CoL^1(OAc)$_2$]	Co(II)/Co(I)	−0.32	−0.56	0.24
[NiL^1(OAc)$_2$]	Ni(II)/Ni(I)	−0.62	−0.82	0.20
[CuL^1(OAc)$_2$]	Cu(II)/Cu(I)	−0.32	−0.16	0.16
[ZnL^1(OAc)$_2$]	Zn(II)/Zn(O)	−0.73	–	–
[CoL^2(OAc)$_2$]	Co(II)/Co(I)	−0.98	−0.82	0.16
[NiL^2(OAc)$_2$]	Ni(II)/Ni(I)	−0.80	−0.58	0.22
[CuL^2(OAc)$_2$]	Cu(II)/Cu(I)	−0.55	−0.37	0.18
[ZnL^2(OAc)$_2$]	Zn(II)/Zn(O)	−0.98	–	–
[CoL^3(OAc)$_2$]	Co(II)/Co(I)	−0.89	−0.76	0.13
[NiL^3(OAc)$_2$]	Ni(II)/Ni(I)	−0.96	−0.84	0.14
[CuL^3(OAc)$_2$]	Cu(II)/Cu(I)	−0.68	−0.59	0.09
[ZnL^3(OAc)$_2$]	Zn(II)/Zn(O)	−0.81	–	–

quasi-reversible Co(II)/Co(I) couple. The anodic peak at $E_{pa} = -0.56$ V *versus* Ag/AgCl and the associated cathodic peak at $E_{pc} = -0.32$ V correspond to the Co(II)/Co(I) couple. The $[CoL^1(OAc)_2]$ complex exhibits quasi-reversible behavior as indicated by the non-equivalent current intensity of cathodic and anodic peaks.

The cyclic voltammogram of $[NiL^1(OAc)_2]$ in acetonitrile at 300 K in the potential range from −0.4 to −1.4 V at a scan rate of 0.1 Vs^{-1} shows a well-defined redox process corresponding to the formation of the quasi-reversible Ni(II)/Ni(I) couple. The anodic peak at $E_{pa} = -0.82$ V *versus* Ag/AgCl and the associated cathodic peak at $E_{pc} = -0.62$ V correspond to the Ni(II)/Ni(I) couple. The $[NiL^1(OAc)_2]$ complex exhibits quasi-reversible behavior as indicated by the non-equivalent current intensity of cathodic and anodic peaks. The high-negative potential shows that the metal ion is highly stabilized by the strong π-donor properties of the substituents which overcomes the π-acceptor property of L^1 [38].

The cyclic voltammogram of $[CuL^1(OAc)_2]$ in acetonitrile at 300 K in the potential range from +0.4 to −0.8 V at a scan rate of 0.1 Vs^{-1}, shown in figure S6 (Supplementary material), shows a well-defined redox process corresponding to the formation of the quasi-reversible Cu(II)/Cu(I) couple. The anodic peak at $E_{pa} = -0.16$ V *versus* Ag/AgCl and the associated cathodic peak at $E_{pc} = -0.32$ V correspond to the Cu(II)/Cu(I) couple. The $[CuL^1(OAc)_2]$ complex exhibits quasi-reversible behavior as indicated by the non-equivalent current intensity of cathodic and anodic peaks [39, 40]. The quasi-reversible behavior of this complex is also supported by the presence of a large peak separation of E_{pa} and E_{pc}. The cyclic voltammogram of $[ZnL^1(OAc)_2]$ in acetonitrile at 300 K in the potential range from −1.3 to +1.7 V at a scan rate of 0.1 Vs^{-1} shows an irreversible peak at −0.728 V, assigned to the Zn(II)/Zn(0) couple.

Similar electrochemical behavior was observed for the Co(II), Ni(II), Cu(II), and Zn(II) complexes of L^2 and L^3 (table 3).

Based on the above results, complexes were assigned structures as shown in figure 1.

3.8. *Antimicrobial activity*

The *in vitro* biological screening effects of the investigated compounds were tested against the bacterial species *S. aureus*, *E. coli*, *K. pneumoniae*, *P. vulgaris*, and

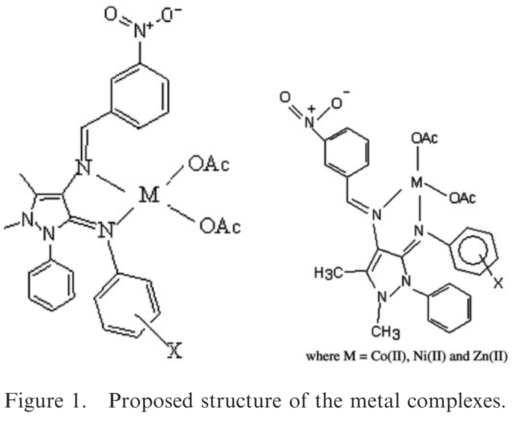

Figure 1. Proposed structure of the metal complexes.

P. aeruginosa and fungal species *A. niger*, *R. stolonifer*, *A. flavus*, *R. bataicola*, and *C. albicans* by the well-diffusion method. The minimum inhibitory concentration (MIC) values of the compounds are summarized in tables 4 and 5. A comparative study of the MIC values for the ligands and their complexes indicates that the complexes exhibit higher antimicrobial activity. Such an increased activity of the complexes can be explained on the basis of Overtone's concept [41] and Tweedy's Chelation theory [42].

3.9. *Effect of substituents*

Generally, the electron withdrawing and electron releasing nature and the position of substituents present in the phenyl ring affect the antimicrobial activities; the presence

Table 4. MIC of the synthesized compounds against growth of bacteria ($\mu g\,mL^{-1}$).

Compound	*E. coli*	*K. pneumoniae*	*P. vulgaris*	*P. aeruginosa*	*S. aureus*
L^1	60	64	66	66	72
$[CoL^1(OAc)_2]$	28	36	26	32	30
$[NiL^1(OAc)_2]$	34	38	32	28	42
$[CuL^1(OAc)_2]$	24	26	20	16	28
$[ZnL^1(OAc)_2]$	26	28	30	26	48
L^2	52	54	58	60	63
$[CoL^2(OAc)_2]$	24	38	28	18	28
$[NiL^2(OAc)_2]$	28	36	34	39	46
$[CuL^2(OAc)_2]$	18	24	14	12	20
$[ZnL^2(OAc)_2]$	32	42	42	28	53
L^3	66	82	68	70	75
$[CoL^3(OAc)_2]$	36	29	36	38	38
$[NiL^3(OAc)_2]$	34	35	40	44	46
$[CuL^3(OAc)_2]$	28	26	38	30	32
$[ZnL^3(OAc)_2]$	32	38	44	48	52
Streptomycin	10	15	6	12	4

Each value observed is within the error limits of ±1.

Table 5. MIC of the synthesized compounds against growth of fungi ($\mu g\,mL^{-1}$).

Compound	*A. niger*	*R. stolonifer*	*A. flavus*	*R. bataicola*	*C. albicans*
L^1	60	66	72	80	50
$[CoL^1(OAc)_2]$	24	28	28	34	30
$[NiL^1(OAc)_2]$	28	30	34	38	32
$[CuL^1(OAc)_2]$	19	20	20	25	22
$[ZnL^1(OAc)_2]$	32	26	46	36	38
L^2	52	55	68	80	50
$[CoL^2(OAc)_2]$	24	25	24	30	25
$[NiL^2(OAc)_2]$	25	36	42	28	30
$[CuL^2(OAc)_2]$	15	14	18	22	20
$[ZnL^2(OAc)_2]$	35	34	38	36	28
L^3	65	58	84	96	74
$[CoL^3(OAc)_2]$	32	36	28	38	36
$[NiL^3(OAc)_2]$	44	38	42	56	38
$[CuL^3(OAc)_2]$	26	30	22	32	28
$[ZnL^3(OAc)_2]$	38	48	48	62	48
Nystatin	10	16	8	14	12

Each value observed is within the error limits of ±1.

of substituents at the *o*-position lowers the antimicrobial activity whereas the substituents at the *m*- and *p*-positions give higher antimicrobial activity. Inhibition is enhanced with the introduction of an electron withdrawing nitro group in the phenyl ring. In the present study, the order of the antimicrobial activity of the synthesized compounds (based on the substituent present in the phenyl ring) is as follows:

$$NO_2 > H > OCH_3$$

The three Schiff-base ligands have higher antimicrobial activity due to the presence of the uncoordinated nitro from 3-nitrobenzaldehyde being present. As pointed above, the higher activity is due to the presence of the two nitro groups situated in the *m*- and *p*-position of the phenyl ring. Among the three Schiff-base ligands, L^2 has higher activity because of the presence of two uncoordinated nitro groups, i.e., one from 3-nitrobenzaldehyde and the other from *p*-nitroaniline. Thus, the order of activity among the three Schiff-base ligands is as follows: $L^2 > L^1 > L^3$.

Supplementary material

Tables S1–S3 and figures S1–S6 are placed in Supplementary material.

References

[1] J.A. McCleverty, T.J. Meyer. *Comprehensive Coordination Chemistry II, from Biology to Nanotechnology*, Vol. 1, p. 411, Elsevier, Amsterdam (2004).
[2] A.D. Garnovskii, I.S. Vasilchenko, D.A. Garnovskii, B.I. Kharisov. *J. Coord. Chem.*, **62**, 151 (2009).
[3] D.M. Boghaei, S. Mohebi. *Tetrahedron*, **58**, 5357 (2002).
[4] A.K. Bhendkar, K. Vijay, A.W. Raut. *Acta Ciencia Indica Chem.*, **30**, 29 (2004).
[5] Y.K. Vaghasiya, R.S. Nair, M. Baluja, S. Chanda. *J. Serb. Chem. Soc.*, **69**, 991 (2004).
[6] K. Vashi, H.B. Naik. *Eur. J. Chem.*, **1**, 272 (2004).
[7] R. Mtrei, M. Yadawe, S.A. Patil. *Orient. J. Chem.*, **12**, 101 (1996).
[8] M.E. Hossain, M.N. Allam, J. Begum, M.A. Akbar, M.N. Uddin, F. Smith, R.C. Hynes. *Inorg. Chim. Acta*, **249**, 207 (1996).
[9] K.P. Sharma V., S. Jolly, P. Phatak. *Ultra. Scient. Phys. Sci.*, **10**, 263 (1998).
[10] V.E. Kuz'min, A.G. Artemenko, R.N. Lozytska, A.S. Fedtchouk, V.P. Lozitsky, E.N. Muratov, A.K. Mescheriakov. *Environ. Res.*, **16**, 219 (2005).
[11] C.T. Barboiu, M. Luca, C. Pop, E. Brewster, M.E. Dinculescu. *Eur. J. Med. Chem.*, **31**, 597 (1996).
[12] N.A. Negm, M.F. Zaki. *Colloids Surf. B: Biointerfaces*, **64**, 179 (2008).
[13] V.P. Daniel, B.S. Kumari, K. Mohanan. *Spectrochim. Acta*, **70A**, 403 (2008).
[14] G. Turan-Zitouni, M. Sivaci, F.S. Kilic, K. Erol. *Eur. J. Med. Chem.*, **36**, 685 (2001).
[15] S.M. Sondhi V., K. Sharma, N. Singhal, R.P. Verma, R. Shukla, R. Raghubir, M.P. Dubey. *Phosphorus, Sulfur Silicon Relat. Elem.*, **156**, 21 (2000).
[16] A.N. Evstopov, V.E. Yavorovskaya, E.S. Vorobev, Z.P. Kudonogova, L.N. Gritsenko, E.N. Schmidt, S.G. Medevedeva V., D. Filimonov, T.P. Prishchep, A.S. Saratikov. *Pharm. Chem. J.*, **26**, 426 (1992).
[17] G.H. Sayed, A. Radwan, S.M. Mohamed, S.A. Shiba, M. Khalil. *Chin. J. Chem.*, **10**, 475 (1992).
[18] G.N. Vassilev, P.A. Yonova, H. Bohland, N.G. Vassilev, B. Yordanov. *Dokl Bulg Akad Nauk*, **50**, 59 (1997).
[19] M. Verleye, I. Heurald, J.M. Gillardin. *Pharmacol. Res.*, **41**, 539 (2000).
[20] N. Raman, S. Johnson Raja, A. Sakthivel. *J. Coord. Chem.*, **62**, 691 (2009).
[21] E.H. Cordes, W.P. Jencks. *J. Am. Chem. Soc.*, **84**, 832 (1962); idem, ibid. **85**, 2843 (1963).
[22] R.J. Angelici. *Synthesis and Techniques in Inorganic Chemistry*, W.B. Saunders Company, Philadelphia, PA (1969).
[23] A.W. Bauer, W.M.M. Kirby, J.C. Sherries, M. Truck. *Am. J. Clin. Pathol.*, **45**, 493 (1996).

[24] W.J. Geary. *Coord. Chem. Rev.*, **7**, 81 (1971).
[25] K. Nakamoto. *Infrared and Raman Spectra of Inorganic and Coordination Compounds*, p. 260, Wiley Interscience, New York (1986).
[26] B. Hammond, F.H. Zardine, A.G. Vohra. *J. Inorg. Nucl. Chem.*, **33**, 1017 (1971).
[27] K.N. Srivastava, S. Das, R.A. Lal. *Indian J. Chem.*, **25(A)**, 85 (1986).
[28] P.B. Sreeja, M.R.P. Kurup. *Spectrochim. Acta*, **61A**, 331 (2005).
[29] A.B.P. Lever. *Inorganic Electronic Spectroscopy*, 2nd Edn, Elsevier, New York (1968).
[30] P.K. Panda, S.B. Mishra, B.K. Mohapatra. *J. Inorg. Chem.*, **42**, 497 (1980).
[31] D.X. West, A.A. Nassar, F.A. El-Saied, M.I. Agad. *Transition Met. Chem.*, **23**, 321 (1988).
[32] E. Canpolat, M. Kaya. *J. Coord. Chem.*, **58**, 1063 (2005).
[33] G.E. Cami, M. Gonzalez Liu, F. Sanaz Ruiz, J.C. Pedregosa. *J. Phys. Chem. Solids*, **66**, 936 (2005).
[34] A. Yazici, F. Akgun. *Transition Met. Chem.*, **31**, 152 (2006).
[35] O. Bastop, C.K. Jorgensen. *Acta Chem. Scand.*, **11**, 1223 (1957).
[36] S.J. Swamy, S. Pola. *Spectrochim. Acta*, **70A**, 929 (2008).
[37] D.E. Billing, B.J. Hathaway, P. Nicholls. *J. Chem. Soc. A*, 316 (1969).
[38] M. Gerloch, J.M. Badarau. *Inorg. Chem.*, **18**, 3226 (1979).
[39] C. Freire, B . De Castro. *J. Chem. Soc., Dalton Trans.*, 1491 (1998).
[40] M. Fujiwara, H. Watika, T. Matsushtla, T. Shono. *Bull. Chem. Soc. Jpn*, **63**, 3443 (1990).
[41] Y. Anjaneyula, R.P. Rao. *Synth. React. Inorg. Met.-Org. Chem.*, **16**, 257 (1986).
[42] N. Dharamaraj, P. Viswanathamurthi, K. Natarajan. *Transition Met. Chem.*, **26**, 105 (2001).